Stem Cell-Containing Hyaluronic Acid-Based Spongy Hydrogels for Integrated Diabetic Wound Healing

Lucília Pereira da Silva[1,2], Tírcia Carlos Santos[1,2], Daniel Barreira Rodrigues[1,2], Rogério Pedro Pirraco[1,2], Mariana Teixeira Cerqueira[1,2], Rui Luís Reis[1,2], Vitor Manuel Correlo[1,2] and Alexandra Pinto Marques[1,2]

The detailed pathophysiology of diabetic foot ulcers is yet to be established and improved treatments are still required. We propose a strategy that directs inflammation, neovascularization, and neoinnervation of diabetic wounds. Aiming to potentiate a relevant secretome for nerve regeneration, stem cells were precultured in hyaluronic acid-based spongy hydrogels under neurogenic/standard media before transplantation into diabetic mice full-thickness wounds. Acellular spongy hydrogels and empty wounds were used as controls. Re-epithelialization was attained 4 weeks after transplantation independently of the test groups, whereas a thicker and more differentiated epidermis was observed for the cellular spongy hydrogels. A switch from the inflammatory to the proliferative phase of wound healing was revealed for all the experimental groups 2 weeks after injury, but a significantly higher M2($CD163^+$)/M1($CD86^+$) subtype ratio was observed in the neurogenic preconditioned group that also failed to promote neoinnervation. A higher number of intraepidermal nerve fibers were observed for the unconditioned group probably due to a more controlled transition from the inflammatory to the proliferative phase. Overall, stem cell-containing spongy hydrogels represent a promising approach to enhance diabetic wound healing by positively impacting re-epithelialization and by modulating the inflammatory response to promote a successful neoinnervation.

Journal of Investigative Dermatology (2017) **137,** 1541–1551; doi:10.1016/j.jid.2017.02.976

INTRODUCTION

Diabetic foot ulcerations (DFUs) are the major cause of nontraumatic foot amputation worldwide (Edwards et al., 2008). Many of these DFUs have associated diabetic peripheral neuropathy that is responsible for an absent sense of touch, pain, and/or temperature due to injured nerves (Laverdet et al., 2015). Diabetic peripheral neuropathy in combination with other factors such as persistent inflammation, impaired re-epithelialization, misbalanced metalloproteinases and tissue inhibitor metalloproteinases levels, and reduced angiogenesis and blood flow have been implicated in the hindered progression of diabetic wound healing (Blakytny and Jude, 2009). Treatment of DFUs with advanced dressings composed of extracellular matrix (e.g., Integra, Integra LifeSciences) or comprising cells and growth factors (e.g., Graftskin/Apligraf, Organogenesis; or Dermagraft, Advanced BioHealing) has been shown to accelerate wound closure (Mulder et al., 2014). Nonetheless, the mechanisms that aid wound healing progression are not clearly understood.

A correlation between DFU healing and diabetic peripheral neuropathy is yet to be established. This is potentially the reason why neuropathy has not been directly targeted in the development of new DFU therapies. So far some works (Kant et al., 2015; Leal et al., 2015; Moura et al., 2014) have targeted the reduced levels of neuromediators in diabetic wounds by delivering neuromediators to the wounds, in order to improve wound re-epithelialization. Others (Blais et al., 2009; Caissie et al., 2006; Gingras et al., 2003) have incorporated Schwann cells into skin tissue-engineered substitutes showing the increased number of nerve fibers, enhanced nerve migration, nerve growth, and myelin sheath formation in the grafted tissues. Despite these interesting results, the isolation and expansion of autologous human Schwann cells for clinical application can be a challenge. Stem cells have been posed as a potential alternative. Nonhuman origin stem cells cultured with a neurogenic cocktail or in coculture with dorsal root ganglia neurons differentiated toward a Schwann cell phenotype display typical functional characteristics of Schwann cells (Caddick et al., 2006; Kingham et al., 2007; Mahay et al., 2008a, 2008b; Tomita et al., 2012). However, the actual

[1]*3B's Research Group—Biomaterials, Biodegradables and Biomimetics, University of Minho, Headquarters of the European Institute of Excellence on Tissue Engineering and Regenerative Medicine, AvePark-Parque da Ciência e Tecnologia, Barco, Taipas, Guimarães, Portugal; and* [2]*ICVS/3B's—PT Government Associate Laboratory, Braga/Guimarães, Portugal*

Correspondence: Alexandra Pinto Marques, 3B's Research Group—Biomaterials, Biodegradables and Biomimetics, University of Minho, Headquarters of the European Institute of Excellence on Tissue Engineering and Regenerative Medicine, AvePark—Parque da Ciência e Tecnologia, Zona Industrial da Gandra, 4805-017 Barco, Taipas, Guimarães, Portugal. E-mail: apmarques@dep.uminho.pt

Abbreviations: BME, β-mercaptoethanol; cond$_A$hASCs, human adipose-derived stem cells conditioned to neurogenic medium A; DFU, diabetic foot ulceration; GG-HA, gellan gum-hyaluronic acid; hASC, human adipose-derived stem cell; RA, retinoic acid

Received 1 September 2016; revised 31 January 2017; accepted 6 February 2017; accepted manuscript published online 1 March 2017

differentiation of human-origin stem cells is still controversial due to the coexpression of glial cell markers and the production of neurotrophic factors by undifferentiated stem cells (Brohlin et al., 2009; Park et al., 2010; Tomita et al., 2013; Tondreau et al., 2004).

Gellan gum spongy hydrogels obtained from gellan gum hydrogels have distinctive properties, including intrinsic cell adhesive characteristics, that have proven beneficial in skin tissue engineering (Cerqueira et al., 2014b; da Silva et al., 2014a, 2014b). When combined with hyaluronic acid, spongy hydrogels also exhibited hyaluronidase-mediated biodegradation that resulted in hyaluronic acid content-dependent neovascularization of ischemic mice hind limb (da Silva et al., 2016). Moreover, an enhanced effect over the neovascularization of excisional skin wound was observed when microvascular endothelial cells and human adipose stem cells (hASCs) were entrapped in gellan gum-hyaluronic acid (GG-HA) spongy hydrogels (Cerqueira et al., 2014b).

In this context, we hypothesized that hASCs preconditioned in neurogenic medium would acquire a Schwann cell-like phenotype with the ability to release neurotrophic factors, which are essential for nerve repair. Thus, hASCs cultured within GG-HA spongy hydrogels in the selected neurogenic conditioning medium would function as a neurotrophic factor-producing platform, ultimately promoting nerve formation in diabetic skin wounds. It was also envisioned that the angiogenic HA fragments released from the spongy hydrogels, associated with the hASCs' capacity to act as a modulator of inflammation, would have an extended effect on balancing the inflammatory state of the wounds. For this purpose, the neurotrophic secretome of hASCs cultured in the standard and neurogenic media was evaluated before entrapment within GG-HA spongy hydrogels. Stem cell-containing GG-HA spongy hydrogels precultured in standard and selected neurogenic conditioning media were implanted in diabetic mice excisional skin wounds, and the capacity of the generated constructs to modulate inflammation and angiogenesis and promote neoinnervation was assessed to confirm the potential of the proposed approach to treat DFUs.

RESULTS

hASCs phenotype and secretome before and after conditioning

In standard culture conditions, hASCs displayed the characteristic mesenchymal stem cell phenotype; more than 90% of the population expressed CD105, CD90, and CD73, and was negative for the hematopoietic markers CD31, CD34, and CD45 (Supplementary Table S1 online). In addition, more than 95% of the hASCs expressed immature (nestin) and mature (glial fibrillary acidic protein, p75, and S100B) glial cell markers (Supplementary Table S1 and Figure 1a), characteristic of neurogenic lineages.

hASCs were preinduced to the neurogenic lineage with β-mercaptoethanol (BME) followed by retinoic acid (RA) exposure, and then induced to a Schwann cell-like phenotype with specific differentiation components and mitogens such as glial growth factor-2, forskolin, platelet-derived growth factor-AA, and basic fibroblast growth factor, following a previously described method (Brohlin et al., 2009), described as neurogenic conditioning medium B. Although this was our reference medium, cells kept proliferating after the preinduction with BME and RA. Thus, to achieve a cell population similarly exposed to BME and RA, these factors were maintained during culture in the presence (medium A) and absence (medium C) of basic fibroblast growth factor, which is responsible for cell proliferation (Figure 1b). Cells exposed to neurogenic conditioning media A and C showed a more polarized morphology in relation to cells cultured in standard and conditioned medium B (Figure 1c). Moreover, when cultured in neurogenic conditioning medium A, the number of cells expressing CD105 and CD73 decreased, respectively, to 75−85% and to 93% (Supplementary Table S1). Independently of the neurogenic conditioning media, no significant changes were observed regarding the expression of the Schwann cell-associated markers nestin, glial fibrillary acidic protein, p75, and S100B (Supplementary Table S1), which were already highly expressed by hASCs. No significant alterations in the secretome of hASCs were detected after the neurogenic conditioning (Figure 1d). However, a tendency for a higher release of brain-derived neurotrophic factor (55.56 ± 30.00 to 31.33 ± 18.85 pg/ml) and ciliary neurotrophic factor (1.67 ± 0.23 to −1.17 ± 0.31 ng/ml) from hASCs cultured in conditioning medium B, and of glial cell-derived neurotrophic factor (47.50 ± 9.92−24.58 ± 3.82 pg/ml) from hASCs in conditioning medium A, relative to unconditioned hASCs was observed (Figure 1d).

The majority of the hASCs entrapped within GG-HA spongy hydrogels were alive and distributed throughout it, colonizing the whole structure along the culture (Figure 1e). Moreover, in the 3D spongy hydrogels, the secretome of the hASCs cultured in the selected conditioned medium A did not change in relation to unconditioned hASCs (Figure 1d).

Wound closure and re-epithelialization

Although wounds were still open 2 weeks after transplantation (Figure 2a), within this period of time, the percentage of wound closure for the GG-HA+hASCS-conditioned to neurogenic medium A ($cond_A$hASCs) condition was higher (83.7 ± 11.2%) than for the GG-HA (56.1 ± 28.2%), GG-HA+hASCs (56.4 ± 23.4%), and control (48.6 ± 19.6%) groups (Figure 2b). As the majority of the wounds were closed 4 weeks after transplantation, wound closure quantification based on the macroscopic images was not performed to avoid inaccurate measurements. Wound re-epithelialization assessment 2 weeks after injury revealed a thin layer of k5 expressing keratinocytes migrating toward the wound center and a thick layer of k10 expressing keratinocytes in the margins for all the conditions (Figure 2c), characteristic of re-epithelialization. At 4 weeks, a thin and fragile epidermis consisting of one to two layers of keratinocytes was observed in the control and GG-HA conditions. In contrast, the wounds treated with cell-containing GG-HA spongy hydrogels presented a well-organized and thicker epidermis with a high number of proliferative keratinocytes in the basal layer, as determined by ki-67 staining (Figure 2c and d).

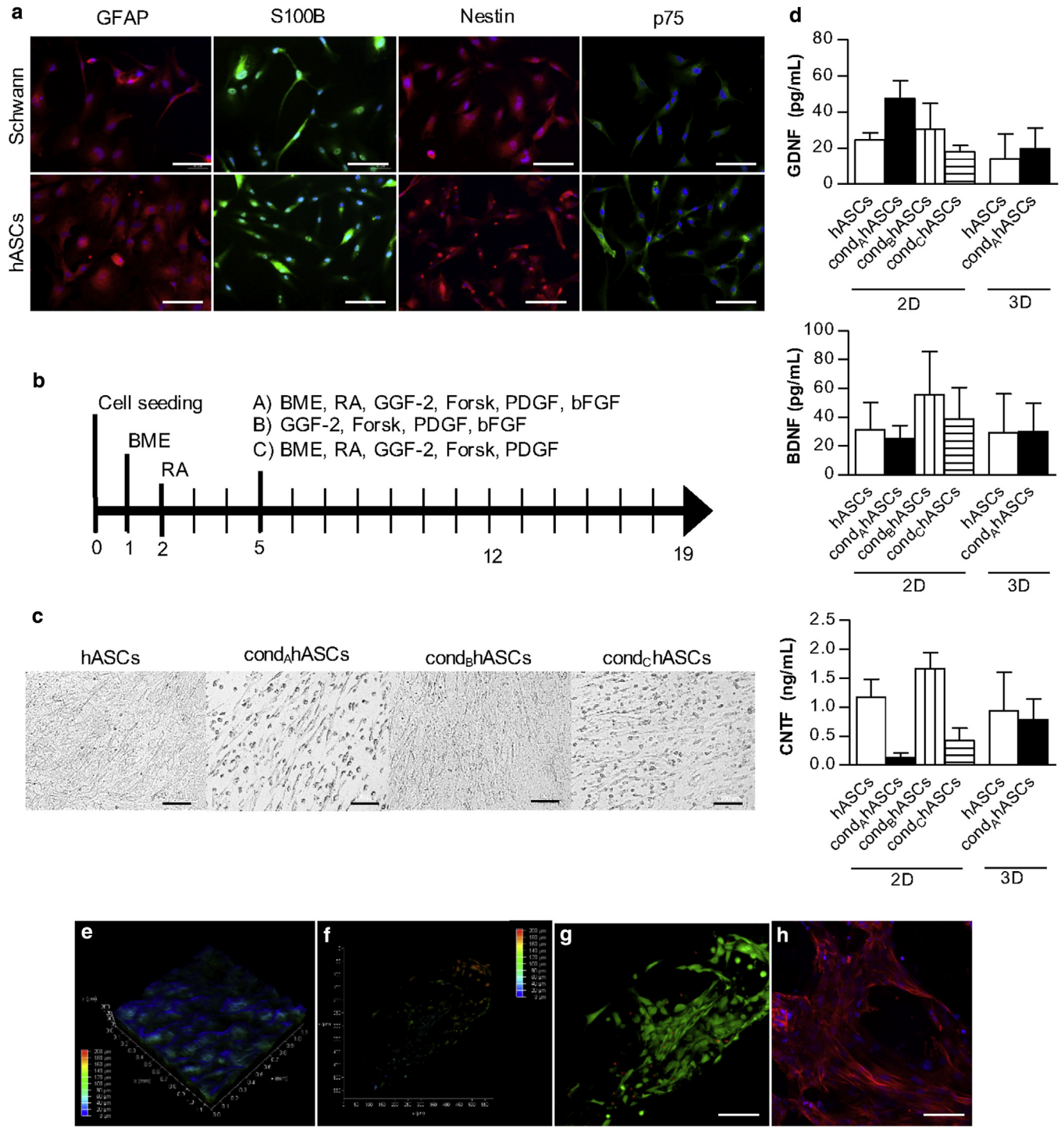

Figure 1. hASC phenotype and secretome. (**a**) Representative immunocytochemistry images of GFAP, S100B, p75, and nestin expression. Nuclei were stained with DAPI (blue). (**b**) hASCs were subjected to conditioning medium A (cond$_A$hASC), B (cond$_B$hASCs), or C (cond$_C$hASCs) for 2 weeks. (**c**) Brightfield representative images of hASCs morphology. (**d**) Amount of neurotrophic factors released by hASCs cultured in standard tissue culture polystyrene and within GG-HA spongy hydrogels. Confocal microscopy representative images of (**e**) GG-HA spongy hydrogels microstructure and (**f**–**h**) hASCs cultured in GG-HA spongy hydrogels for 21 days evidencing cell (**f**) distribution, (**g**) viability (calcein—green, propidium iodide—red), and (**h**) spreading (phalloidin—red, DAPI—blue). Scale bar = 100 μm. BDNF, brain-derived neurotrophic factor; bFGF, basic fibroblast growth factor; BME, β-mercaptoethanol; CNTF, ciliary neurotrophic factor; cond$_A$hASC, human adipose-derived stem cells conditioned to neurogenic medium A; Forsk, forskolin; GDNF, glial cell-derived neurotrophic factor; GFAP, glial fibrillary acidic protein; GGF-2, glial growth factor-2; GG-HA, gellan gum-hyaluronic acid; PDGF, platelet-derived growth factor; RA, retinoic acid.

Inflammatory host response

GG-HA spongy hydrogels were well integrated in the wound site 2 weeks after transplantation (Figure 3 and Supplementary Figure S1 online). The presence of an inflammatory exudate that infiltrated the GG-HA spongy hydrogels was observed at week 2 independently of the condition, but it was almost absent at week 4 (Figure 3 and Supplementary Figure S1), confirming the progression of the

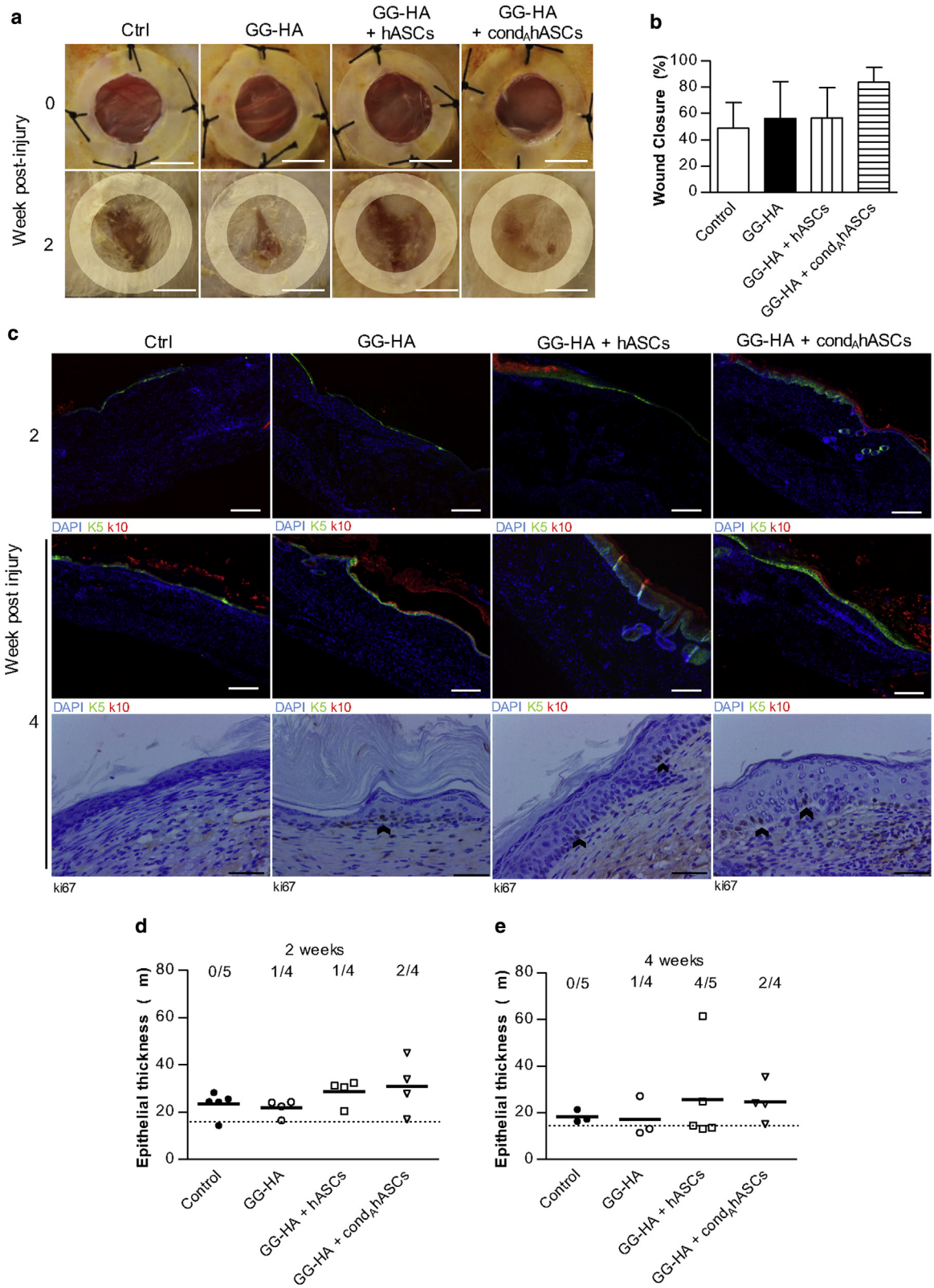

Figure 2. Wound closure and re-epithelialization 2 and 4 weeks after transplantation of GG-HA, GG-HA+hASCs, and GG-HA+cond$_A$hASCs into diabetic mice full-thickness wounds. (**a**) Representative images of the wounds and (**b**) respective percentage of wound closure. Scale bar = 5 mm. Control corresponds to an empty wound. (**c**) Representative immunohistochemistry images of k5, k10 (scale bar = 200 μm), and ki-67 (scale bar = 50 μm) expression in the wound center. Epidermis thickness quantification in the wound center (**d**) 2 and (**e**) 4 weeks after transplantation. Each measurement represents the average for each animal, and the dashed line represents the average of diabetic mice skin. On the top of the symbols is indicated the total of re-epithelialized wounds per analyzed animals. cond$_A$hASCs, human adipose-derived stem cells conditioned to neurogenic medium A; GG-HA, gellan gum-hyaluronic acid.

healing cascade. Matrix deposition and organization was improved in the presence of GG-HA spongy hydrogels less, irregularly distributed collagen deposition was observed for the control, whereas a more organized collagenous dermis was observed for all the other conditions. Moreover, the material was barely detected 4 weeks after injury, only small fragments being perceived in the middle of the dermis (Figure 3 and Supplementary Figure S1), which demonstrated that the material degradation did not negatively influence healing. The observed inflammatory infiltrate was largely composed of macrophages (Figure 4a). Significantly higher ($P < 0.001$) percentages of $CD163^+$ anti-inflammatory macrophages were observed in nontreated wounds (21.63 ± 14.59%, control), in comparison with all the other conditions (16.97 ± 12.79%, GG-HA+hASCs; 10.52 ± 11.67%, GG-HA+cond$_A$hASCs) except for the higher percentage of $CD163^+$ cells (28.06 ± 19.39%) observed in the GG-HA group (Figure 4b). Moreover, significantly lower ($P < 0.001$) percentages were observed for GG-HA+cond$_A$hASCs than for the GG-HA and GG-HA+hASCs conditions, as well as for GG-HA+hASCs in comparison with GG-HA. The presence of $CD86^+$ proinflammatory macrophages was also significantly lower ($P < 0.001$) for all the groups (11.26 ± 12.73%, GG-HA; 11.82 ± 16.24%, GG-HA+hASCs; 1.1 ± 2.2%, GG-HA+cond$_A$hASCs) relative to the control (24.49 ± 19.71%) (Figure 4c). Moreover, significantly lower ($P < 0.001$) percentages were observed for GG-HA+cond$_A$hASCs in comparison with GG-HA and GG-HA+hASCs. A significantly higher ($P < 0.05$) $CD163^+/CD86^+$ ratio was observed for the wounds treated with GG-HA+cond$_A$hASCs in relation to the control, demonstrating a switch from the inflammatory to the proliferative phase of healing (Figure 4d).

Neovascularization and neoinnervation

Neovascularization was not very different among the tested conditions (Figure 5a), except for the significantly higher ($P < 0.001$) vessel density observed for the GG-HA condition in relation to the control, both at 2 and 4 weeks after transplantation (Figure 5b).

The analysis of the expression of protein gene product 9.5 (Figure 6a) revealed that most of the nerves in the epidermis of the control and GG-HA conditions were swollen and discontinuous in opposition to the longer and continuous nerves found in the epidermis of the wounds treated with cell-containing GG-HA spongy hydrogels in particular for the GG-HA+hASCs group (Figure 6a). Moreover, a higher number of intraepidermal nerve fibers were quantified in the epidermis of the wounds of the GG-HA+hASCs group (Figure 6b). A reduced presence of Remak bundles with lower number of axons was also observed in the dermis of the control condition in relation to the other groups (Figure 6a).

DISCUSSION

Although in patients with nonassociated pathologies, the origin of impaired skin healing is mainly caused by external factors—most commonly infection and pressure—non-healing diabetic skin wounds are further linked to specific factors, such as persistent inflammation, impaired re-epithelialization, misbalanced levels of metalloproteases, and tissue inhibitor metalloproteases (TIMPs), and reduced angiogenesis and blood flow (Falanga, 2005). The use of stem cells to treat diabetic wounds has been showing promise (Heublein et al., 2015). Although the correlation between the diabetic peripheral neuropathy (Pittenger et al., 2004), the decline of angiogenic molecules (Beer et al., 1997; Bruhn-Olszewska et al., 2012; Luo and Chen, 2005; Quattrini et al., 2008; Thangarajah et al., 2009), and the reduced endothelial progenitor cell proliferation and homing to the injury site (Costa and Soares, 2013) is yet to be established, it might be one way to explore the development of new therapies. Considering this, the known hASC features (Glenn and Whartenby, 2014; Wang et al., 2014), and our previous results with hASCs-containing GG-HA spongy hydrogels in terms of neovascularization of skin wounds (Cerqueira et al., 2014a, 2014b), we propose an integrated tissue engineering strategy that modulates inflammation and angiogenesis, and promotes neoinnervation of diabetic wounds.

The implantation of GG-HA spongy hydrogels into diabetic mice full-thickness wounds elicited similar effects to those previously observed by us in a nondiabetic excisional wound model (Cerqueira et al., 2014a, 2014b). Fundamentally, GG-HA spongy hydrogels accelerated wound closure in relation to control, whereas the incorporation of hASCs, including in the GG-HA+cond$_A$hASCs condition considered in this work, lead to an increase in the thickness of the neoepidermis relative to the GG-HA. Considering the high number of proliferative keratinocytes observed in the basal layer of the fully stratified neoepidermis, this effect of the hASCs seems to tackle one of the issues of diabetic keratinocytes, which, although highly proliferative, fail to differentiate (Jude et al., 2002; Usui et al., 2008), thus fostering re-epithelialization. These results are in agreement with others that similarly showed that stem cell-containing hydrogels accelerated wound closure (Kim et al., 2016; Xu et al., 2013) and increased neoepidermis thickness (Xu et al., 2013) in relation to the control. The ability of GG-HA spongy hydrogels to decrease the amount of macrophages in the wound site and prompt a switch from the inflammatory to the proliferative phase of wound healing was demonstrated by the higher ratio of anti-inflammatory M2 ($CD163^+$) to proinflammatory M1 ($CD86^+$) macrophages, encountered 2 weeks after injury. From the few works that have focused on this analysis, N-isopropylacrylamide hydrogels were also shown to significantly reduce, at days 5−7 after treatment, the amount of $CD86^+$ macrophages in Leprdb type II diabetic mice excisional wounds (Chen et al., 2015). Moreover, a diminished incidence of mononuclear cells (Upadhyay et al., 2014), in particular macrophages (Reyes-Ortega et al., 2015), has also been observed in hydrogels with antioxidant and/or anti-inflammatory properties. Hence, the observed progression of the healing cascade in the GG-HA group seems to be related to a direct effect of HA fragments on macrophages, which was previously shown to activate an NF-kB/I-KBα autoregulatory loop in murine macrophages (da Silva et al., 2015; Jiang et al., 2007; Noble, 1996), inducing that phenotype switch. Interestingly, improved outcomes were observed for the GG-HA+hASCs condition, as demonstrated by the higher M2/M1 macrophage ratio in

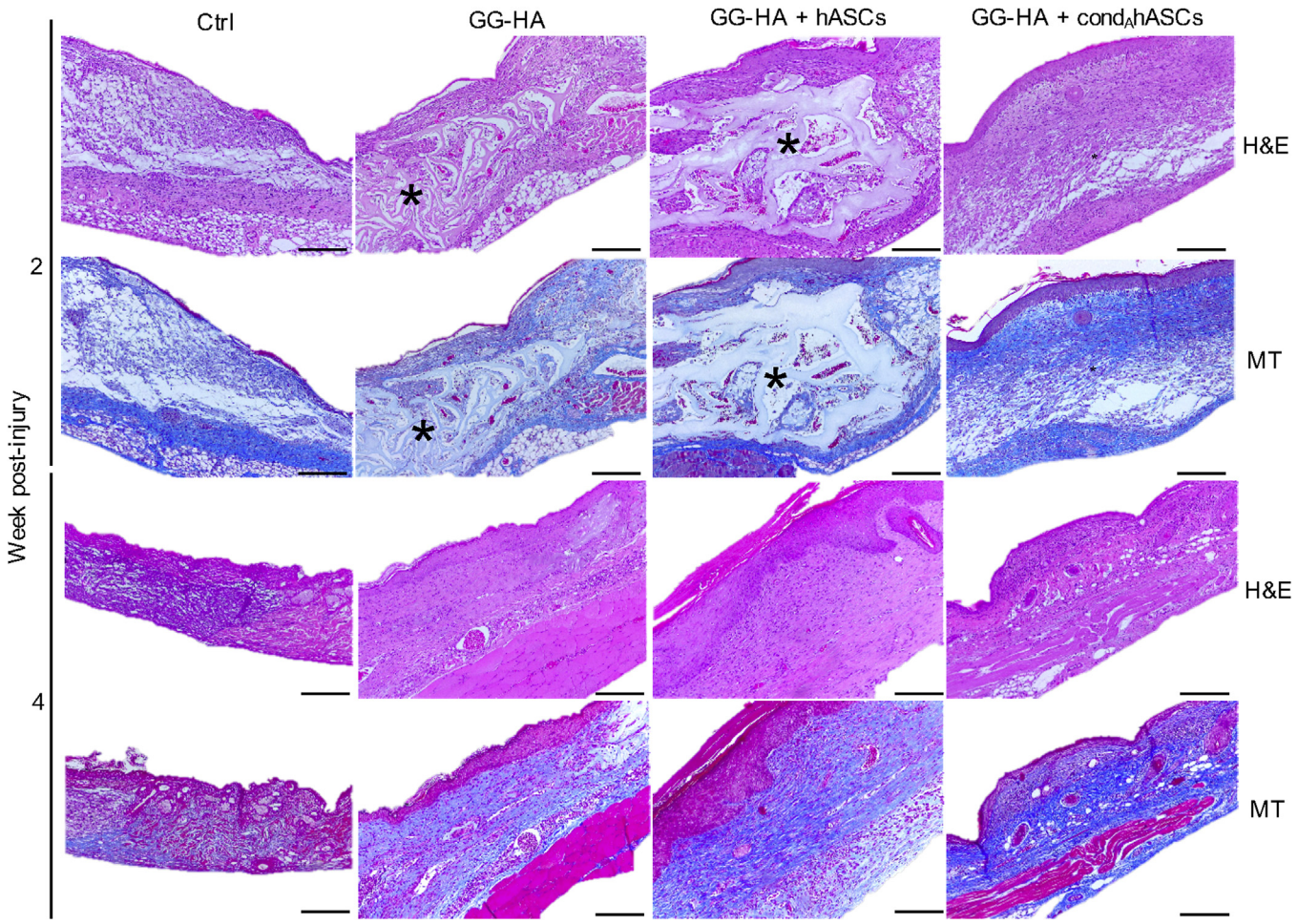

Figure 3. Representative H&E and Masson's Trichrome images 2 and 4 weeks after transplantation of GG-HA, GG-HA+hASCs, and GG-HA+cond$_A$hASCs into diabetic mice full-thickness wounds. Control corresponds to empty wound. *GG-HA spongy hydrogel. Scale bar = 200 μm. cond$_A$hASCs, human adipose-derived stem cells conditioned to neurogenic medium A; GG-HA, gellan gum-hyaluronic acid; H&E, hematoxylin and eosin; MT, Masson's trichrome.

relation to the GG-HA condition, evidencing an advanced state of resolution of the inflammatory phase. To our knowledge, this is the first reported evidence of additional macrophage polarization elicited by stem cells in hydrogels, because the outcomes attained by other works (Chen et al., 2015; Xu et al., 2013) were comparable with the respective control. This can be explained by the capability of GG-HA spongy hydrogels to support the adhesion of hASCs, potentiating their modulatory secretome through the release of inflammatory mediators, such as IL-6, granulocyte macrophage colony-stimulating factor, and prostaglandin E2, that are known to play a role in the M1 to M2 switch (Glenn and Whartenby, 2014). Furthermore, an even higher M2/M1 macrophage ratio was observed for the GG-HA+cond$_A$hASCs condition. This can be related to residual RA, used in the neurogenic conditioning medium, and which has been used to suppress inflammation in chronic inflammatory diseases (Stevison et al., 2015). The accelerated resolution of the inflammatory phase observed for the stem cell-containing GG-HA spongy hydrogel groups relative to the GG-HA condition is also in agreement with the diminished vessel density observed for those groups. Considering the reduced angiogenesis and blood flow (Siperstein et al., 1968), the inactivation and diminished chemoattraction of immune cells, and reduced release of inflammatory mediators (Bruhn-Olszewska et al., 2012; Maruyama et al., 2007; Naghibi et al., 1987; Zykova et al., 2000) that lead to the resolution of persistent inflammation in diabetic nonhealing wounds, these results can be of major significance for the development of improved therapies. The differentiation potential of stem cells toward a Schwann cell-like phenotype is a current subject of research due to the difficulties in isolating and expanding human Schwann cells. However, the expression of Schwann cell phenotypic markers by hASCs and the similar neurotrophic secretome (Brohlin et al., 2009; Park et al., 2010; Tomita et al., 2013; Tondreau et al., 2004) raises several issues regarding the differentiation of these cells into a nerve-regenerating lineage. We postulated that the conditioning of hASCs with neurogenic medium before transplantation would benefit nerve repair mainly due to their secretome, which was shown to be enriched in glial cell-derived neurotrophic factor in 2D cultures. This was however not confirmed in the precultured 3D spongy hydrogels that correlate with the failure of our hypothesis and the absence of a superior neoinnervation in the GG-HA+cond$_A$hASCs condition. Nonetheless, higher

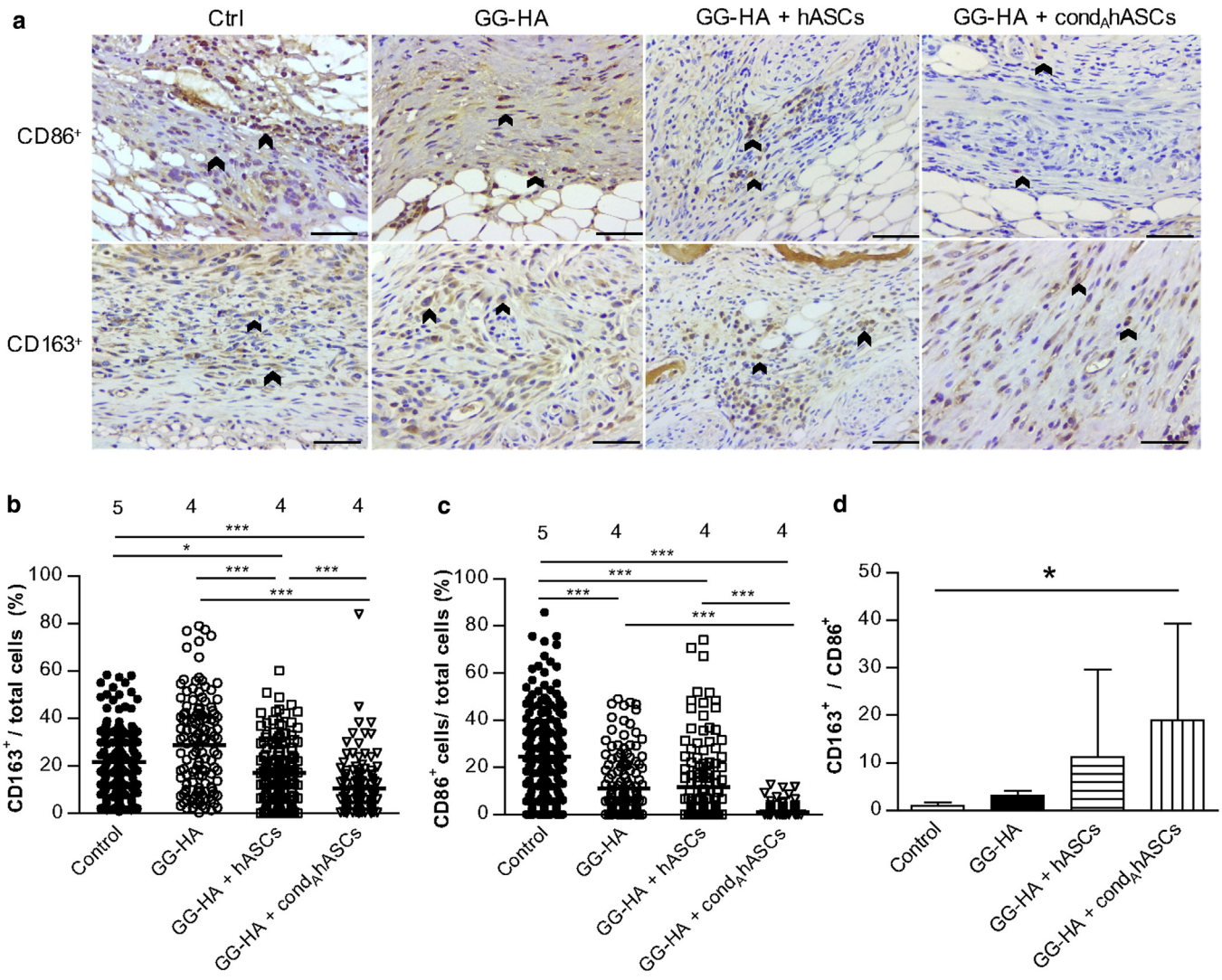

Figure 4. Macrophage recruitment and polarization 2 weeks after transplantation of GG-HA, GG-HA + hASCs, and GG-HA + cond$_A$hASCs into diabetic mice full-thickness wounds. Control corresponds to empty wound. (**a**) Representative immunohistochemistry images against CD86 and CD163 (arrow heads) and quantification of the percentage of (**b**) $CD163^+$ and (**c**) $CD86^+$ cells, and (**d**) respective ratio. Each symbol represents the percentage of positive cells quantified in each acquired image. On top of the symbols the total number of analyzed animals is identified (*$P < 0.05$, ***$P < 0.001$, relative to control). Scale bar = 50 μm. cond$_A$hASCs, human adipose-derived stem cells conditioned to neurogenic medium A; GG-HA, gellan gum-hyaluronic acid.

intraepidermal nerve fiber values were obtained in the GG-HA+hASCs, in agreement with other works that similarly reported the beneficial effects of stem cells in the treatment of peripheral neuropathy (Fairbairn et al., 2015; Han et al., 2015; Sowa et al., 2016). The differences observed between the GG-HA+cond$_A$hASCs and GG-HA+hASCs conditions might be associated with the amount of neurotrophic factors released by inflammatory cells that were reported to significantly improve nerve repair (Elkabes et al., 1996; Hikawa and Takenaka, 1996), demonstrating a beneficial effect in modulating inflammation over axon regeneration (Benowitz and Popovich, 2011).

Diabetic wound etiology requires a new therapeutic approach. Herein we propose an integrated approach that promotes healing but more importantly allows modulating wound neovascularization and inflammation hyaluronic acid that seems to positively impact neoinnervation.

MATERIALS AND METHODS

Preparation of hyaluronic acid-based spongy hydrogels

GG-HA spongy hydrogels were prepared from GG-HA hydrogels after freezing and freeze-drying, as previously described with some modifications (da Silva et al., 2014b) and indicated in the Supplementary Materials and Methods online.

Cell isolation, culture, and neurogenic conditioning

hASCs were obtained from Hospital da Prelada (Porto, Portugal), after patients' written, informed consent and under a collaboration protocol with the 3B's Research Group, approved by the ethical committees of both institutions. Fat tissue was harvested from lipoaspirates of three independent healthy donors who underwent abdominoplasties and processed to isolate hASCs, as previously described (Cerqueira et al., 2013). Human NF1 Schwann-Like cells (sNF96.2) were purchased from ATCC and routinely cultured under the conditions defined by the company. Neurogenic conditioning

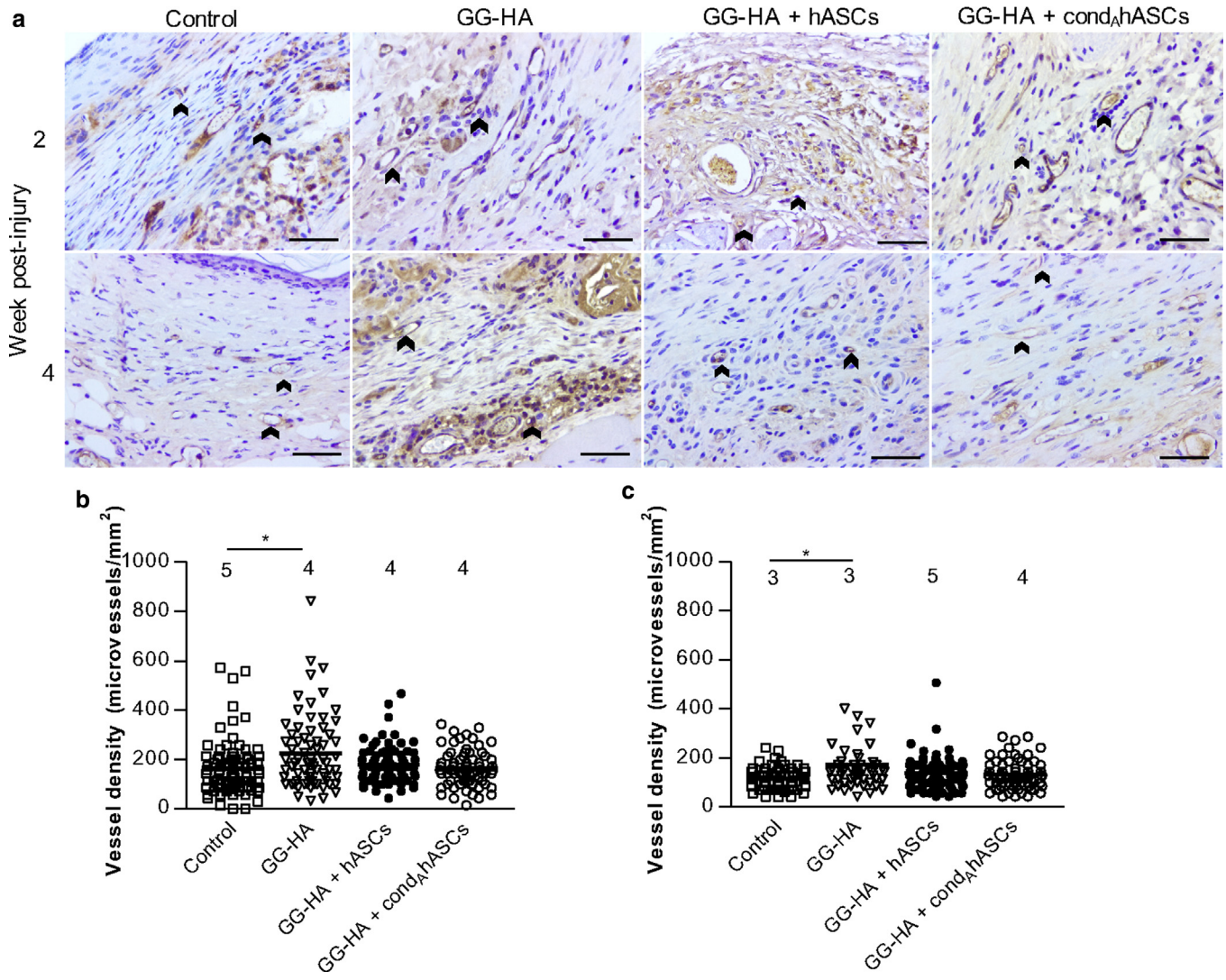

Figure 5. Neovascularization 2 and 4 weeks after transplantation of GG-HA, GG-HA+hASCs, and GG-HA+cond$_A$hASCs into diabetic mice full-thickness wounds. (**a**) Representative images of 2 and 4 weeks' tissue sections immunostained against CD31 (arrow heads). Vessel density quantification (**b**) 2 and (**c**) 4 weeks after injury, based on CD31 staining. Each symbol represents the vessel density quantified in each acquired image. On top of the symbols the total number of analyzed animals is identified (*$P < 0.05$, relative to control). Scale bar = 50 μm. cond$_A$hASCs, human adipose-derived stem cells conditioned to neurogenic medium A; GG-HA, gellan gum-hyaluronic acid.

was induced in hASCs at passage 1, as previously described (Brohlin et al., 2009), with some modifications. Briefly, hASCs (2,000 cells/cm^2) were seeded on culture plates, and after overnight adhesion, α-MEM (standard medium) containing 1 mM of BME (Life Technologies, UK) was added to the cells for 24 hours. Growth medium was then replaced by α-MEM supplemented with 35 ng/ml of RA (Sigma) for 72 hours. Cells were then cultured in α-MEM supplemented with: (i) 126 ng/ml glial growth factor-2 (abcam), 14 μM of forskolin (Sigma), 5 ng/ml of platelet-derived growth factor-AA (Peprotech), 10 ng/ml of basic fibroblast growth factor (Peprotech), 1 mM of BME, and 35 ng/ml of RA; (ii) medium A without RA and BME; or (iii) medium A without basic fibroblast growth factor. Media changes were performed every 72 hours. Cell morphology was followed using an inverted microscope (Axio Observer, Zeiss, Germany).

Diabetic full-thickness excisional wound model

The implantation procedure was approved by the Direcção Geral de Alimentação Veterinária, the Portuguese National Authority for Animal Health, and all the surgical procedures respected the national regulations and international animal welfare rules. Type I diabetes was induced in male mice (CD1-ICR from Charles River, France) by administration of multiple low doses (45 mg/kg) of streptozotocin (Sigma), according to preexisting protocols (Furman, 2015; O'Brien et al., 2014). After establishing type I diabetes (≥250 mg/dl of glucose), animals were maintained for 3 weeks to stabilize diabetes and neuropathy progression (Homs et al., 2011). Mice were divided into 4 groups: (i) empty wound—control; (ii) spongy hydrogels—GG-HA; (iii) spongy hydrogels with hASCs precultured in standard culture medium—GG-HA+hASCs; (iv) spongy hydrogels with hASCs precultured in neurogenic conditioning medium A—GG-HA+cond$_A$hASCs. A total of 60 animals, 5 animals per condition and per time point (2, 4, and 8 weeks), were used. A 9-mm Ø skin full-thickness excision was created and a donut-shaped 9-mm silicone splint (ATOS Medical, Sweden) was placed around the wound to minimize wound contraction. After transplantation of the constructs, wounds were successively covered with Normlgel,

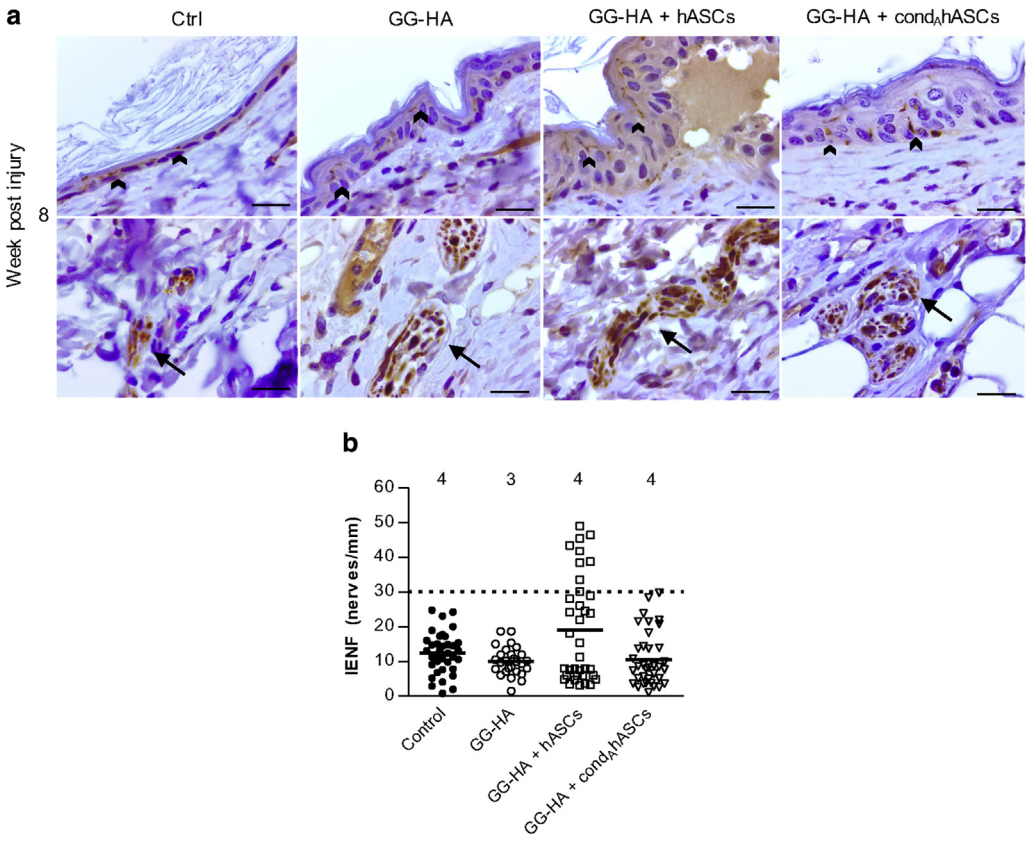

Figure 6. Neoinnervation of the epidermis 8 weeks after transplantation of GG-HA, GG-HA + hASCs, and GG-HA + cond$_A$hASCs into diabetic mice full-thickness wounds. (**a**) Representative immunohistochemistry images against PGP 9.5 evidencing nerve endings (arrow heads) and Remak bundles (arrows) and respective (**b**) intraepidermal nerve fiber quantification. Each symbol represents the value of IENF quantified for each animal, and the dashed line represents IENF average of diabetic mice skin. Scale bar = 20 μm. cond$_A$hASCs, human adipose-derived stem cells conditioned to neurogenic medium A; GG-HA, gellan gum-hyaluronic acid; IENF, intraepidermal nerve fibers; PGP, protein gene product.

Tegaderm transparent dressing, and Omnifix. Animals were left to recover and then kept with food and drinking water ad libitum.

Immunocytochemistry and immunohistochemistry

For immunocytochemistry, cells were incubated with rabbit antihuman S100B (1:200, Dako, Denmark), mouse antihuman nestin (1:50, R&D Systems), mouse antihuman p75 (1:50, Santa Cruz), and mouse antihuman glial fibrillary acidic protein (abcam, UK) primary antibodies overnight at 4 °C. For immunohistochemistry, rabbit antimouse CD31 (abcam), rabbit antimouse CD86 (Bioss Antibodies), rabbit antimouse CD163 (Bioss Antibodies), rabbit antimouse K5 (Covance), mouse antimouse K10 (abcam), rabbit antimouse ki67 (abcam), and protein gene product 9.5 (abcam) were the primary antibodies used. Cells/sections were then incubated with the secondary antibodies Alexa Fluor 488 or 594, or the universal Alexa Fluor secondary antibody from the R.T.U. VECTASTAIN Elite ABC Kit (Vector Labs). The peroxidase substrate kit (DAB, Vector Labs) was used according to the manufacturer's instructions. The Mouse on Mouse Detection kit (Vector Labs) was used according to the manufacturer's instructions for the protein gene product 9.5 identification. Nuclei were stained with hematoxylin (BioOptica, Italy) or DAPI (Biotium). Tissue sections were observed using an Axioimager Z1m microscope (Zeiss) using Zen 2012 software or Microscope Leica DM750 (Germany).

Quantification analysis

Wound closure, CD163 and CD86 positive cells, microvessel density, and intraepidermal nerve fiber quantification details are included in Supplementary Materials and Methods.

Statistical analysis

GraphPad software was used to perform statistical analysis. Data were analyzed by the Shapiro-Wilk normality test. Data with a normal distribution were analyzed using one-way analysis of variance with Tukey's posttest or Dunnett's posttest; data that did not follow a normal distribution were analyzed by the Kruskal-Wallis test with Dunn's multiple comparison posttest. Significance was set to $^*P < 0.05$, $^{**}P < 0.01$, $^{***}P < 0.001$. Results are presented as mean ± standard deviation.

CONFLICT OF INTEREST

The authors state no conflict of interest.

ACKNOWLEDGMENTS

The authors would like to acknowledge Gene2Skin Project (H2020-TWINN-2015-692221) and Fundação para a Ciência e Tecnologia for SFRH/BD/78025/2011 (LPdS), SFRH/BPD/96611/2013 (MTC), SFRH/BPD/101886/2014 (RPP), SFRH/BPD/101952/2014 (TCS) grants. Moreover, the authors would also like to acknowledge Teresa Oliveira for histology support, Andreia Carvalho for hASCs supply, Luca Gasperini for cell profiler analysis, and Manuela E. L. Lago and Carla M. Abreu for intraepidermal nerve fiber quantification.

SUPPLEMENTARY MATERIAL

Supplementary material is linked to the online version of the paper at www.jidonline.org, and at http://dx.doi.org/10.1016/j.jid.2017.02.976.

REFERENCES

Beer H-D, Longaker MT, Werner S. Reduced expression of PDGF and PDGF receptors during impaired wound healing. J Invest Dermatol 1997;109:132–8.

Benowitz LI, Popovich PG. Inflammation and axon regeneration. Curr Opin Neurol 2011;24:577–83.

Blais M, Grenier M, Berthod F. Improvement of nerve regeneration in tissue-engineered skin enriched with schwann cells. J Invest Dermatol 2009;129:2895–900.

Blakytny R, Jude EB. Altered molecular mechanisms of diabetic foot ulcers. Int J Low Extrem Wounds 2009;8:95–104.

Brohlin M, Mahay D, Novikov LN, Terenghi G, Wiberg M, Shawcross SG, et al. Characterisation of human mesenchymal stem cells following differentiation into Schwann cell-like cells. Neurosci Res 2009;64:41–9.

Bruhn-Olszewska B, Korzon-Burakowska A, Gabig-Cimińska M, Olszewski P, Węgrzyn A, Jakóbkiewicz-Banecka J. Molecular factors involved in the development of diabetic foot syndrome. Acta Biochim Pol 2012;59:507–13.

Caddick J, Kingham PJ, Gardiner NJ, Wiberg M, Terenghi G. Phenotypic and functional characteristics of mesenchymal stem cells differentiated along a Schwann cell lineage. Glia 2006;54:840–9.

Caissie R, Gingras M, Champigny M-F, Berthod F. In vivo enhancement of sensory perception recovery in a tissue-engineered skin enriched with laminin. Biomaterials 2006;27:2988–93.

Cerqueira MT, da Silva LP, Santos TC, Pirraco RP, Correlo VM, Marques AP, et al. Human skin cell fractions fail to self-organize within a gellan gum/hyaluronic acid matrix but positively influence early wound healing. Tissue Eng Part A 2014a;20:1369–78.

Cerqueira MT, da Silva LP, Santos TC, Pirraco RP, Correlo VM, Reis RL, et al. Gellan gum-hyaluronic acid spongy-like hydrogels and cells from adipose tissue synergize promoting neoskin vascularization. ACS Appl Mater Interfaces 2014b;6:19668–79.

Cerqueira MT, Pirraco RP, Santos TC, Rodrigues DB, Frias AM, Martins AR, et al. Human adipose stem cells cell sheet constructs impact epidermal morphogenesis in full-thickness excisional wounds. Biomacromolecules 2013;14:3997–4008.

Chen S, Shi J, Zhang M, Chen Y, Wang X, Zhang L, et al. Mesenchymal stem cell-laden anti-inflammatory hydrogel enhances diabetic wound healing. Sci Rep 2015;5:18104.

Costa PZ, Soares R. Neovascularization in diabetes and its complications. Unraveling the angiogenic paradox. Life Sci 2013;92:1037–45.

da Silva LP, Cerqueira MC, Pirraco RP, Santos TC, Reis RL, Correlo VM, et al. Gellan gum-hyaluronate spongy-like hydrogels promote angiogenesis in hindlimb ischemia. 4th TERMIS World Congr. Boston, MA, Tissue Eng. Part A. 2015;21(Suppl. 1):S-1–S-413.

da Silva LP, Cerqueira MT, Sousa RA, Marques AP, Correlo VM, Reis RL. Gellan gum-based spongy-like hydrogels: methods and biomedical applications thereof. US patent US20160325017 A1. 2014a.

da Silva LP, Cerqueira MT, Sousa RA, Reis RL, Correlo VM, Marques AP. Engineering cell-adhesive gellan gum spongy-like hydrogels for regenerative medicine purposes. Acta Biomater 2014b;10:4787–97.

da Silva LP, Pirraco RP, Santos TC, Novoa-Carballal R, Cerqueira MT, Reis RL, et al. Neovascularization induced by the hyaluronic acid-based spongy-like hydrogels degradation products. ACS Appl Mater Interfaces 2016;8:33464–74.

Edwards JL, Vincent AM, Cheng HT, Feldman EL, Edwards JL, Vincent AM, et al. Diabetic neuropathy: Mechanisms to management. Pharmacol Ther 2008;120:1–34.

Elkabes S, DiCicco-Bloom EM, Black IB. Brain microglia/macrophages express neurotrophins that selectively regulate microglial proliferation and function. J Neurosci 1996;16:2508–21.

Fairbairn NG, Meppelink AM, Ng-Glazier J, Randolph MA, Winograd JM. Augmenting peripheral nerve regeneration using stem cells: a review of current opinion. World J Stem Cells 2015;7:11–26.

Falanga V. Wound healing and its impairment in the diabetic foot. Lancet 2005;366:1736–43.

Furman BL. Streptozotocin-induced diabetic models in mice and rats. Curr Protoc Pharmacol 2015;70:1–20.

Gingras M, Paradis I, Berthod F. Nerve regeneration in a collagen-chitosan tissue-engineered skin transplanted on nude mice. Biomaterials 2003;24:1653–61.

Glenn JD, Whartenby KA. Mesenchymal stem cells: emerging mechanisms of immunomodulation and therapy. World J Stem Cells 2014;6:526–39.

Han JW, Choi D, Lee MY, Huh YH, Yoon YS. Bone marrow-derived mesenchymal stem cells improve diabetic neuropathy by direct modulation of both angiogenesis and myelination in peripheral nerves. Cell Transpl 2015;25:1–38.

Heublein H, Bader A, Giri S. Preclinical and clinical evidence for stem cell therapies as treatment for diabetic wounds. Drug Discov Today 2015;20:703–17.

Hikawa N, Takenaka T. Myelin-stimulated macrophages release neurotrophic factors for adult dorsal root ganglion neurons in culture. Cell Mol Neurobiol 1996;16:517–28.

Homs J, Ariza L, Pagès G, Verdú E, Casals L, Udina E, et al. Comparative study of peripheral neuropathy and nerve regeneration in NOD and ICR diabetic mice. J Peripher Nerv Syst 2011;16:213–27.

Jiang D, Liang J, Noble PW. Hyaluronan in tissue injury and repair. Annu Rev Cell Dev Biol 2007;23:435–61.

Jude EB, Blakytny R, Bulmer J, Boulton AJM, Ferguson MWJ. Transforming growth factor-beta 1, 2, 3 and receptor type I and II in diabetic foot ulcers. Diabet Med 2002;19:440–7.

Kant V, Kumar D, Kumar D, Prasad R, Gopal A, Pathak NN, et al. Topical application of substance P promotes wound healing in streptozotocin-induced diabetic rats. Cytokine 2015;73:144–55.

Kim EJ, Choi JS, Kim JS, Choi YC, Cho YW. Injectable and thermosensitive soluble extracellular matrix and methylcellulose hydrogels for stem cell delivery in skin wounds. Biomacromolecules 2016;17:4–11.

Kingham PJ, Kalbermatten DF, Mahay D, Armstrong SJ, Wiberg M, Terenghi G. Adipose-derived stem cells differentiate into a Schwann cell phenotype and promote neurite outgrowth in vitro. Exp Neurol 2007;207:267–74.

Laverdet B, Danigo A, Girard D, Magy L, Demiot C, Desmoulière A. Skin innervation: important roles during normal and pathological cutaneous repair. Histol Histopathol 2015;30:875–92.

Leal EC, Carvalho EE, Tellechea A, Kafanas A, Tecilazich F, Kearney C, et al. Substance P promotes wound healing in diabetes by modulating inflammation and macrophage phenotype. Am J Pathol 2015;185:1638–48.

Luo JD, Chen AF. Nitric oxide: a newly discovered function on wound healing. Acta Pharmacol Sin 2005;26:259–64.

Mahay D, Terenghi G, Shawcross SG. Schwann cell mediated trophic effects by differentiated mesenchymal stem cells. Exp Cell Res 2008a;314:2692–701.

Mahay D, Terenghi G, Shawcross SG. Growth factors in mesenchymal stem cells following glial-cell differentiation. Biotechnol Appl Biochem 2008b;51:167.

Maruyama K, Asai J, Ii M, Thorne T, Losordo DW, D'Amore PA. Decreased macrophage number and activation lead to reduced lymphatic vessel formation and contribute to impaired diabetic wound healing. Am J Pathol 2007;170:1178–91.

Moura LIF, Dias AMA, Suesca E, Casadiegos S, Leal EC, Fontanilla MR, et al. Neurotensin-loaded collagen dressings reduce inflammation and improve wound healing in diabetic mice. Biochim Biophys Acta 2014;1842:32–43.

Mulder G, Tenenhaus M, D'Souza GF. Reduction of diabetic foot ulcer healing times through use of advanced treatment modalities. Int J Low Extrem Wounds 2014;13:335–46.

Naghibi M, Smith RP, Baltch AL, Gates SA, Wu DH, Hammer MC, et al. The effect of diabetes mellitus on chemotactic and bactericidal activity of human polymorphonuclear leukocytes. Diabetes Res Clin Pract 1987;4:27–35.

Noble PW. Hyaluronan fragments activate an NF-kappa B/I-kappa B alpha autoregulatory loop in murine macrophages. J Exp Med 1996;183:2373–8.

O'Brien PD, Sakowski SA, Feldman EL. Mouse models of diabetic neuropathy. ILAR J 2014;54:259–72.

Park H-W, Lim M-J, Jung H, Lee S-P, Paik K-S, Chang M-S. Human mesenchymal stem cell-derived Schwann cell-like cells exhibit neurotrophic effects, via distinct growth factor production, in a model of spinal cord injury. Glia 2010;58:1118–32.

Pittenger GL, Ray M, Burcus NI, McNulty P, Basta B, Vinik AI. Intraepidermal nerve fibers are indicators of small-fiber neuropathy in both diabetic and nondiabetic patients. Diabetes Care 2004;27:1974–9.

Quattrini C, Jeziorska M, Boulton AJM, Malik RA. Reduced vascular endothelial growth factor expression and intra-epidermal nerve fiber loss in human diabetic neuropathy. Diabetes Care 2008;31:140–5.

Reyes-Ortega F, Cifuentes A, Rodríguez G, Aguilar MR, González-Gómez Á, Solis R, et al. Bioactive bilayered dressing for compromised epidermal

tissue regeneration with sequential activity of complementary agents. Acta Biomater 2015;23:103–15.

Siperstein MD, Unger RH, Madison LL. Studies of muscle capillary basement membranes in normal subjects, diabetic, and prediabetic patients. J Clin Invest 1968;47:1973–99.

Sowa Y, Kishida T, Imura T, Numajiri T, Nishino K, Tabata Y, et al. Adipose-derived stem cells promote peripheral nerve regeneration in vivo without differentiation into Schwann-like lineage. Plast Reconstr Surg 2016;137:318e–30e.

Stevison F, Jing J, Tripathy S, Isoherranen N. Role of retinoic acid-metabolizing cytochrome P450s, CYP26, in inflammation and cancer. Adv Pharmacol 2015;74:373–412.

Thangarajah H, Yao D, Chang EI, Shi Y, Jazayeri L, Vial IN, et al. The molecular basis for impaired hypoxia-induced VEGF expression in diabetic tissues. Proc Natl Acad Sci USA 2009;106:13505–10.

Tomita K, Madura T, Mantovani C, Terenghi G. Differentiated adipose-derived stem cells promote myelination and enhance functional recovery in a rat model of chronic denervation. J Neurosci Res 2012;90:1392–402.

Tomita K, Madura T, Sakai Y, Yano K, Terenghi G, Hosokawa K. Glial differentiation of human adipose-derived stem cells: implications for cell-based transplantation therapy. Neuroscience 2013;236:55–65.

Tondreau T, Lagneaux L, Dejeneffe M, Massy M, Mortier C, Delforge A, et al. Bone marrow–derived mesenchymal stem cells already express specific neural proteins before any differentiation. Differentiation 2004;72:319–26.

Upadhyay A, Chattopadhyay P, Goyary D, Mitra Mazumder P, Veer V. Ixora coccinea enhances cutaneous wound healing by upregulating the expression of collagen and basic fibroblast growth factor. ISRN Pharmacol 2014;2014:751824.

Usui ML, Mansbridge JN, Carter WG, Fujita M, Olerud JE. Keratinocyte migration, proliferation, and differentiation in chronic ulcers from patients with diabetes and normal wounds. J Histochem Cytochem 2008;56:687–96.

Wang Y, Chen X, Cao W, Shi Y. Plasticity of mesenchymal stem cells in immunomodulation: pathological and therapeutic implications. Nat Immunol 2014;15:1009–16.

Xu K, Cantu DA, Fu Y, Kim J, Zheng X, Hematti P, et al. Thiol-ene Michael-type formation of gelatin/poly(ethylene glycol) biomatrices for three-dimensional mesenchymal stromal/stem cell administration to cutaneous wounds. Acta Biomater 2013;9:8802–14.

Zykova SN, Jenssen TG, Berdal M, Olsen R, Myklebust R, Seljelid R. Altered cytokine and nitric oxide secretion in vitro by macrophages from diabetic type II-like db/db mice. Diabetes 2000;49:1451–8.